Cement & Concrete Composites 44 (2013) 30–40

Contents lists available at SciVerse ScienceDirect

Cement & Concrete Composites

journal homepage: www.elsevier.com/locate/cemconcomp

Development of cement-based lightweight composites – Part 2: Durability-related properties

P. Spiesz *, Q.L. Yu, H.J.H. Brouwers

Department of the Built Environment, Eindhoven University of Technology, P.O. Box 513, 5600 MB Eindhoven, The Netherlands

ARTICLE INFO

Article history:
Received 21 March 2012
Received in revised form 16 January 2013
Accepted 22 March 2013
Available online 17 April 2013

Keywords:
Cement-based lightweight composites
Recycled expanded glass
Porosity
Durability
Transport properties

ABSTRACT

Cement-based lightweight composites were developed in Part 1 of this study [1], employing the modified Andreasen and Andersen particle packing model. The design was targeted on a good balance between the mechanical and thermo-physical performance of the material. By the application of expanded glass lightweight aggregates in a form of closed spheres, the design was also targeted on a low permeability to fluids, which is a unique feature for this type of material. The durability-related properties of the developed lightweight composites were investigated in this paper. The durability was quantified based on the measurements of water-permeable porosity, capillary water absorption, chloride transport properties, electrical resistivity, freeze–thaw resistance and alkali-silica reaction. The results show that by using the proposed design methodology, it is possible to develop lightweight composites of low density and thermal conductivity, sufficient strength and low permeability to fluids.

1. Introduction

As stated by Neville [2], in the past there was a predominating trend of thinking that 'strong concrete is durable concrete'. However, the strength and durability of concrete usually have to be considered individually in the design stage. It is not difficult to imagine how in different environments 'strong' concrete may fail due to an improper design of its durability. The durability of concrete in most cases is actually related to its permeability (or more precisely penetrability) to fluids. The permeability is a resultant of many factors such as the permeable porosity of the hardened cement paste and aggregates and the quality of aggregate/cement paste interface. On the one hand, at high permeability, aggressive substances can easily penetrate into the concrete, facilitating its deterioration. On the other hand, an increased porosity and permeability often help to resist the damage caused by freeze–thaw or the expandable products of the alkali-silica reaction. According to Neville [2], there are three fluids relevant to durability which can penetrate into concrete and cause its deterioration: water (pure or carrying deleterious ions), oxygen and carbon dioxide. Their transport from the surrounding environment into concrete takes place through the pores. The conventional (normal density) concrete constitutes the major part of the worldwide concrete production, and therefore it focuses the largest part of the carried-out research. Hence, the durability and related transport properties of this type of concrete attract most of the attention and have already been intensively investigated in literature.

One type of concrete that has not been thoroughly analyzed in terms of durability is lightweight concrete. Due to the lack in the knowledge, often there is a strong unwillingness to use lightweight concrete as it is expected to be more permeable (and less durable as a result) compared to normal density concretes. Thus, the main focus of the present study is the analysis of transport properties of fluids in lightweight cement-based materials. This transport, due to an increased porosity of the lightweight materials, could be significantly facilitated compared to normal density concrete.

Because of its low density and good thermal insulation, lightweight aggregates (LWAs) concrete is an attractive material for certain fields of application such as walls of houses and offices, tall buildings or off-shore structures. Due to their large porosity, the lightweight aggregates can potentially be very permeable, significantly increasing the overall permeability of the composite containing these LWA. This potential is reflected by the connectivity of the internal pores of the LWA to the surrounding matrix. Most of the LWA available on the market for mass production of concrete have high open porosity. However, there are also LWA with closed pores, originating from their special production process. One example of such LWA are expanded glass lightweight aggregates produced from recycled glass. Such aggregates are composed of a closed external shell which encapsulates a number of internal

* Corresponding author. Tel.: +31 (0)40 247 5904; fax: +31 (0)40 243 8595.
E-mail address: p.spiesz@tue.nl (P. Spiesz).

0958-9465/$ - see front matter © 2013 Elsevier Ltd. All rights reserved.
http://dx.doi.org/10.1016/j.cemconcomp.2013.03.029

Nomenclature

a^2	cross-section area of the sample (mm^2)
C_A	capillary water absorption index (g/mm^2)
C_t	total chloride content ($g_{Cl}/100\ g_{mortar}$)
D_{app}	apparent chloride diffusion coefficient (m^2/s)
D_{RCM}	chloride migration coefficient (m^2/s)
f	frequency (Hz)
m_0	initial mass of the sample (g)
m_{28}	mass of the sample after 28 days of exposure to water (g)
R	electrical resistivity (Ωm)
S_n	surface scaling of mortar samples due to freeze–thaw cycles (g/m^2)
φ_{LWA}	volume fraction of LWA in the mixture (dm^3/m^3)
φ_{paste}	volume fraction of cement paste in the mixture (dm^3/m^3)
φ_v	volume fraction of voids (%)
$\varphi_{v,LWA}$	volume fraction of voids in the mixture of LWA (%)
$\varphi_{v,p}$	volume fraction of water-permeable voids (%)
$\varphi_{v,paste}$	volume fraction of voids in cement paste (%)
$\varphi_{v,paste'}$	volume fraction of voids in the cement paste including the void fraction contributed by 0.1–0.3 mm LWA (%)

air pores. This internal cellular structure with a closed external shell can be seen in Fig. 1. Therefore, an increased porosity introduced by the LWA does not necessarily have to cause an increased permeability of the produced lightweight composite. This is demonstrated in Fig. 2 [3], where the possible interrelations between the porosity and permeability are shown. However, as commonly known, not only the type of used aggregates influences the permeability of concrete/mortar, but also the quality of the cement paste, air content and the aggregate/paste interface. Thus, in order to produce a lightweight material with low permeability, it is of vital importance to combine together proper LWA (closed porosity and/or low interconnectivity of the internal pores) with a dense hardened cement paste (low water/cement ratio), well bound to the aggregates.

By far, the available design methodologies for lightweight concrete are targeted only on low density (thermal conductivity) or good strength, without taking into account its permeability. The permeability of concrete or mortar is determined by its porosity and connectivity of the pores. In the case of LWA composites, the porosity is very high and often coupled with an increased interconnectivity of the pores. In turn, lightweight composites very often have increased permeability. Liu et al. [4] found that the transport properties of LWA concrete such as water absorption, permeability coefficient and resistance to chloride penetration are more closely related to the water-permeable porosity than to the total porosity of concrete. However, contradicting conclusions were presented by Chia and Zhang [5], who stated that the resistance against chloride penetration of LWA concrete is not related to its permeability to water. In [5,6] it was shown that the LWA sand causes significant increase on the permeability of concrete compared to normal density sand. Additionally, in [4,5] it was found that the capillary porosity of the hardened cement plays a much more significant role in the transport of fluids than the porosity of the LWA. Some studies [4,7,8] also show that the permeability of LWA concrete could be even lower than that of normal density concrete prepared with similar w/c ratios and attribute this to the internal curing effect of the LWA pre-soaked in water and to the better quality of the ITZ.

In Part 1 of this study [1] a mix design methodology based on the modified Andreasen & Andersen particle packing model was applied for the design of LWA cement-based composites. The followed design approach is based on the high packing density of the granular solid ingredients. Hence, the developed LWA mortars are expected to have low permeabilities, especially when the internal LWA pores remain closed. As shown in Part 1 [1], this mix design methodology provides an attractive tool to design lightweight materials and can be targeted on a good balance between their mechanical properties (compressive and flexural strengths), density and thermal conductivity or focus only on one target property. As the mechanical and thermo-physical properties of the developed composites were presented in Part 1 of this study [1], the investigations on the durability-related properties are addressed in this article. Therefore, the porosity, water transport properties (capillary water absorption, depth of penetration of water under pressure and freeze–thaw resistance), chloride transport properties (accelerated and natural chloride intrusion) and possibility of the alkali-silica reaction are analyzed here. Thus, this paper will investigate whether the applied concrete design methodology can be used also to develop a lightweight material with low permeability, which would be a unique feature. Additionally, based on the performed experiments and data retrieved from literature, the relationship between the permeability and porosity will be analyzed for a broad scope of porosities (densities) of concretes and mortars.

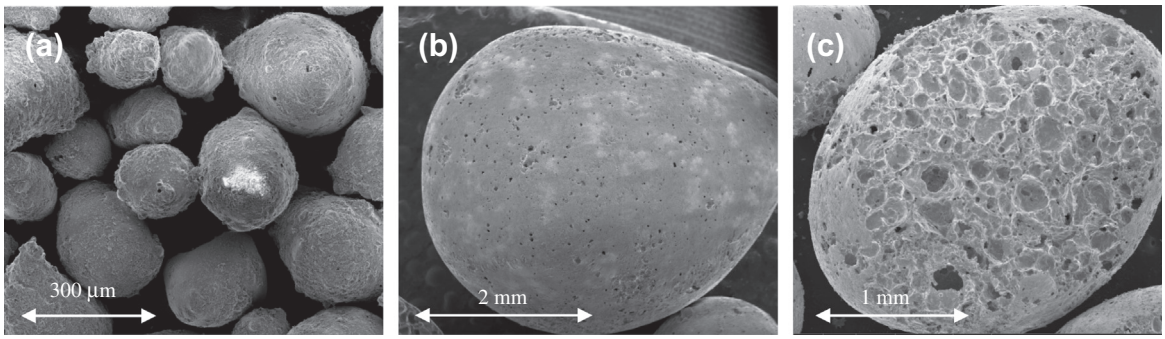

Fig. 1. SEM pictures of the external surface of (a) LWA 0.1–0.3 mm, (b) LWA 2–4 mm and (c) the internal fracture surface of LWA 1–2 mm.

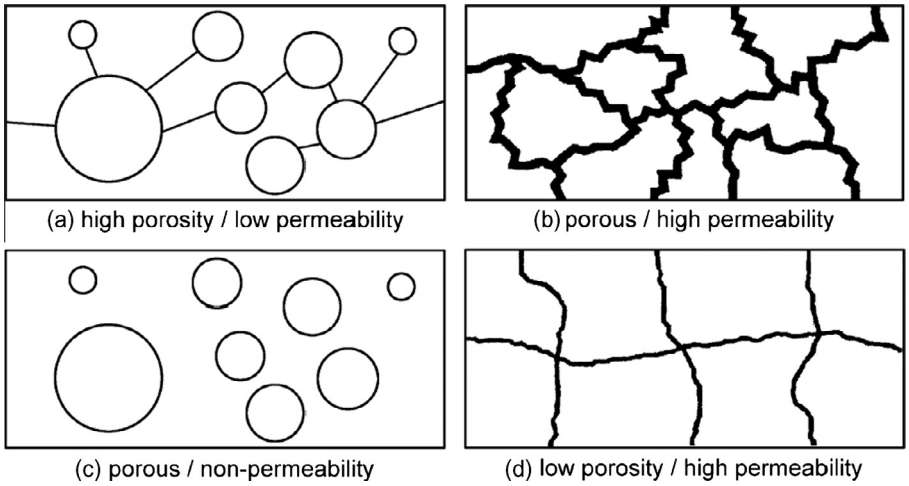

Fig. 2. Possible interrelations between porosity and permeability [3].

2. Experimental

A summary of the composition of the LWA composites developed in Part 1 [1] is given in Table 1, where SCLC1 and SCLC2 represent the self-compacting lightweight composites and VCLC is the conventional (vibrated) lightweight composite. As can be seen, five different size fractions of the expanded glass LWA were used. However, for the VCLC only the coarser fraction of the LWA were applied (1–2 mm and 2–4 mm) and the finer fractions were replaced by normal density sand (conventional sand 0–4 mm and microsand 0–1 mm, containing high amounts of fine particles). To ensure a sufficient workability of both self-compacting mortars, larger amounts of fine materials were used (limestone powder, microsand and LWA in the size range of 0.1–0.3 mm). For the strength tests as well as for the capillary water absorption test $40 \times 40 \times 160\ mm^3$ prisms were cast, while for the porosity, water penetration, chloride ingress and the freeze–thaw tests, cubes of $150 \times 150 \times 150\ mm^3$ were cast. One day after casting, all the specimens were de-molded and stored at 100% relative humidity (RH) until the testing period. A detailed description of the properties of the used materials, mix design method, properties of the lightweight mortars in fresh state (flowability, density) and in hardened state (mechanical and thermo-physical properties) are presented in Part 1 of this study [1].

Table 1
Mix proportions of mortars.

Material	SCLC1 (kg/m^3)	SCLC2 (kg/m^3)	VCLC (kg/m^3)
CEM I 52.5 N	425.3	423.5	419.7
Limestone powder	111.9	259.6	0.0
Sand 0–4 mm	0.0	0.0	407.0
Sand 0–1 mm	0.0	95.6	0.0
Microsand	381.5	424.6	306.0
LWA 0.1–0.3 mm	56.0	68.3	0.0
LWA 0.25–0.5 mm	44.8	0.0	0.0
LWA 0.5–1.0 mm	56.0	54.9	0.0
LWA 1.0–2.0 mm	44.8	39.4	63.6
LWA 2.0–4.0 mm	0.0	0.0	71.6
Water	250.9	230.3	159.4
Superplasticizer (wt.% of cement)	1.0	1.0	0.8
Water/cement ratio	0.59	0.54	0.38
Water/powder[a] ratio	0.35	0.26	0.29
Dry density (kg/m^3)	1280	1490	1460
Thermal conductivity (W/(m K))	0.485	0.738	0.847
28 Days compressive strength (N/mm^2)	23.3	30.2	27.5

[a] Particles smaller than 125 μm.

2.1. Test methods

2.1.1. Water-permeable porosity

Three disks (height of 10–15 mm, diameter of 100 mm), extracted from the inner layers of three 150 mm cubes for each type of developed composite, were used to determine the water-permeable porosity. The treatment of the samples was carried out following the procedure described in [9,10], performing the saturation of the samples with water under vacuum conditions (applied pressure of 40 mbar). The vacuum-saturation was applied, as this technique is reported to be the most efficient [11]. The water-permeable porosity of the samples was calculated following the description presented in [12] and more details are given in Part 1 of this article [1].

2.1.2. Penetration of water under pressure

The depth of the penetration of water under pressure was tested at the age of 28 days according to [13]. The samples (three 150 mm cubes for each prepared mix) were exposed to water under the pressure of 5 bars for 72 h and subsequently split in order to measure the maximum depth of the water penetration front. When a leakage of water from the side wall of a cube was observed, the test on that cube was terminated.

2.1.3. Capillary water absorption

The water capillary absorption test was performed following the procedure described in [14]. Six prisms ($40 \times 40 \times 160\ mm^3$) for each mix were tested. After a 28 days curing period the prisms were positioned vertically in a container covered with a lid. About 3 mm of the bottom of the samples were immersed in water. The level of water was adjusted every 72 h. The capillary water absorption test was performed for 54 days, during which the mass of the samples was recorded periodically.

2.1.4. Freeze–thaw resistance

The freeze–thaw resistance of the LWA mortars was determined following [15]. The test samples differed from the specifications given in the standard – for practical reasons cylindrical samples were used instead of slabs. The 150 mm cubes after demolding were cured at 100% RH until the age of 25 days, when the cores

(100 mm in diameter) were extracted by drilling and sliced (two cylinders of 50 mm in height were obtained from each core). Subsequently, the cylinders were clamped in rubber sleeves, placed in polyurethane insulations of 10 mm thickness and surface-saturated with demineralised water for 3 days. Due to a limited volume of the climate chamber, three specimens were tested for each mix, resulting in a total exposed surface area of 0.024 m^2 (the area recommended in [15] is 0.08 m^2). After the saturation, the freeze-thaw test was carried out with a 3 mm layer of de-mineralized water poured on the top surface. The temperature profile in the chamber followed the recommendations given in [15]. The level of water on the surface of the samples was adjusted regularly. In total, 56 freeze–thaw cycles were applied, during which the surface scaling was measured after 14, 28 and 56 cycles.

2.1.5. SEM analysis

Samples of the LWA aggregates and hardened composites were analyzed using a high resolution scanning electron microscope (FEI Quanta 600 FEG-SEM) with a Schottky field emitter gun (at voltage of 2–10 keV) in high- and low-vacuum modes. The obtained pictures were used to investigate the microstructure of the developed LWA composites as well as the presence of alkali-silica reaction.

2.1.6. Resistivity

The electrical resistance of cylindrical samples (diameter of 100 mm, height of 150 mm), saturated under vacuum-conditions with limewater, was measured using the 'two electrodes' method [16] at the age of 28 days. A scheme of the test set-up is shown in Fig. 3. An AC test signal (f = 1 kHz) was applied between the two stainless-steel electrodes and the resistance of the mortar specimen placed between the electrodes and wet sponges was measured using a digital LCR meter. During the measurement a 2 kg load was applied on the upper electrode to eliminate drifts of the test signal. Finally, from the measured resistance, the resistivity of the samples was calculated by taking their thicknesses and transversal areas into account. After the measurements, the same samples were further used for the Rapid Chloride Migration test.

2.1.7. Rapid Chloride Migration (RCM) test

For each developed mixture three cores (diameter of 100 mm, height of 150 mm) were extracted from different cubes. Two specimens for the RCM test were retrieved from each core, giving in total six test specimens (cylinders with a diameter of 100 mm and height of 50 mm) for each mix. Three of these specimens were tested at the age of 28 days and the other three at 91 days. One day prior to the RCM test, the specimens were pre-conditioned (vacuum-saturation with limewater), following the same procedure as described for the measurements of water-permeable porosity in Part 1 [1]. The RCM test was performed according to [9], using the test set-up and procedure described in [17]. The duration of the RCM test for all the samples was 24 h. After the test, the penetration depth of chlorides was measured in split samples by applying a colourimetric indicator for chlorides (0.1 mol/dm^3 $AgNO_3$ solution) and subsequently, the chloride migration coefficient (D_{RCM}) was calculated following [9].

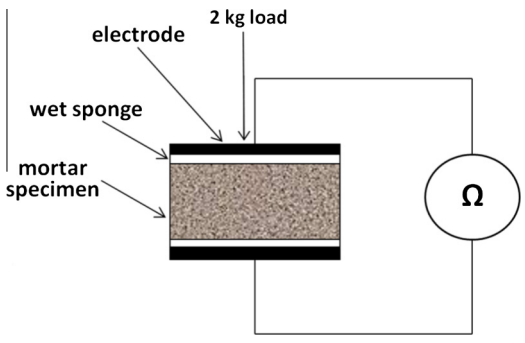

Fig. 3. Test set-up for the measurement of electrical resistance.

2.1.8. Chloride diffusion test

For each prepared mix, three specimens (cylinders, diameter of 100 mm and height of 50 mm) were extracted from different cubes. The diffusion test was performed on 28 days old samples, following the procedure described in [18]. Prior to the test, all external faces of the specimens were coated with an epoxy resin except for one flat surface, left uncovered to allow the chlorides to penetrate into the samples just from that side. Then, the specimens were immersed in a sodium chloride solution (concentration of 165 g/dm^3) for 63 days, at room temperature, in a sealed and de-aired container, with the uncoated surface on top. After the exposure period, one specimen from each test series was split in order to measure the penetration depth of chlorides, using 0.1 mol/dm^3 $AgNO_3$ solution as a colourimetric chloride indicator. The remaining samples were dry-ground in layers for the determination of the chloride concentration profiles. The grinding was performed on an area of 73 mm in diameter. The obtained powder was collected for the determination of the total chloride concentration profiles, following the procedure given in [19]. An automatic potentiometric titration unit was used for the Cl^- concentration measurements, employing a 0.01 mol/dm^3 $AgNO_3$ solution as the titrant. In order to estimate the apparent chloride diffusion coefficient (D_{app}) and the surface total-chloride concentration, the solution of Fick's 2nd law was fit to the measured total-chloride concentration profile, as described in [18]. In the curve fitting procedure, performed using the Solver function in MS Excel, the unknown parameters were derived.

3. Results and discussion

3.1. Total and water-permeable porosity

Lightweight concrete/mortars normally are highly porous. Their high porosities are caused not only by the capillary pores of the hardened cement paste, microcracks or air bubbles introduced during mixing, but mainly by the highly porous LWA and air bubbles generated artificially by adding air-entraining or foaming agents. The latter two additives generate a great number of well interconnected air bubbles in the paste matrix of concrete/mortar. The composites produced in this way have very high porosities and are very permeable. In the case of the LWA used in this study, a large fraction of the internal LWA pores may remain encapsulated within the external shell of the LWA. In this way, the produced composite may be highly porous, but still retain low interconnectivity of the pores and, as a result, low permeability. Prior to the measurements of the water-permeable porosities of the mortars, their total porosities were estimated. This could give an indication on the fraction of the internal LWA pores remaining closed.

Detailed information about the measurement and calculation of the volume fraction of permeable voids (water-permeable porosity) is presented in Part 1 of this study [1]. The obtained values of the water-permeable porosity ($\varphi_{v,p}$) are shown in Table 2. One can notice that for both self-compacting composites (SCLC1 and SCLC2) the permeable porosities are comparable, while for the vibrated composite (VCLC) it is slightly lower. However, all the obtained values are much larger compared to conventional normal density concrete or mortar (about 10–15% by volume), which can be attributed to the large internal porosity of the lightweight

aggregates. Although the external shell of the used expanded glass LWA is rather closed and impermeable, it still contains some openings (see Fig. 1), through which liquids can enter into the aggregates. The inflow of water into the LWA is more significant during the process of the vacuum-saturation with water, applied for the measurements of the water-permeable porosity, which was also observed in [20].

The total void fraction (total porosity) φ_v of each developed composite consists of the porosities contributed individually by the hardened cement paste ($\varphi_{v,paste}$) and LWA ($\varphi_{v,LWA}$), taking into account the volumes of the cement paste (φ_{paste}) and the LWA (φ_{LWA}) in the mixture. The estimated porosities and volumes can be found in Table 2. The porosity of the hardened cement paste was calculated in Part 1 of this study [1], using the method proposed by Brouwers [21,22], which is based on the Powers and Brownyard cement hydration model [23]. The porosity of different LWA applied in the developed composites was computed by taking into account the porosity and amount of each individual LWA size fraction (see [1]).

Despite the significant differences between the total porosities of the developed LWA composites (range of 38–47%), their water-permeable porosities are quite similar (range of 30–35%), as shown in Table 2. Assuming the capillary pores completely saturated with water after performing the vacuum-saturation, the difference between the measured permeable porosity ($\varphi_{v,p}$) and the estimated total porosity (φ_v) gives an indication of the amount of the closed pores introduced to the composite by the LWA. All the measured values of the water-permeable porosities are smaller than the calculated total porosities, as listed in Table 2. This indicates that some of the internal LWA pores in the samples remain closed, i.e. not accessible to the penetrating water. As can be also seen in Table 2, the estimated total porosity of SCLC1 is much larger than that of SCLC2, but the measured water-permeable porosities of these two mortars are similar, about 35%. This shows that a significant fraction of internal pores of LWA in mix SCLC1 remains closed, while in mix SCLC2 they are mostly interconnected (i.e. permeable). The water/cement ratios of both self-compacting mortars were comparable, and therefore their estimated capillary porosities ($\varphi_{v,paste}$) are also similar (see Table 2). This difference in the permeabilities can be linked to the amount of the finest size fraction of the LWA (0.1–0.3 mm), which was larger in SCLC2 compared to SCLC1. Apparently, the finest LWA fractions could be penetrated by water easier than the coarser fractions, probably because the distance that water has to travel within the LWA is shorter. This size effect means that the probability of reaching a dead-end pore that hinders any further transport of water is lower in smaller particles. The larger amount of the fine LWA applied in SCLC2 apparently increases the permeability of the paste, and in turn of the entire composite. As can be seen in Table 2, the $\varphi_{v,p}$ measured for the vibrated LWA composite is lower than that of the self-compacting mortars. Despite the lowest mass content of LWA in VCLC mixture among the three developed composites, the volumetric content of LWA in VCLC mixture is the largest (φ_{LWA} in Table 2), as the coarse size fractions of LWA applied in VCLC are more porous compared to the finer fractions applied in SCLC1 and SCLC2. When comparing the water-permeable and the total porosities of VCLC, one can notice that there is a significant fraction of the internal LWA pores that remain closed. This can be attributed to the good quality (low porosity) of the cement paste, and to the application of only coarse LWA size fractions (size effect). Hence, it can be concluded that the combined effects of low water/cement ratio and the absence of the finest fraction of the LWA in mix VCLC reduced its water-permeable porosity significantly. On the other hand, the permeability of both self-compacting mortars was higher, and this can be attributed to the high porosity of the hardened cement paste and to the application of fine LWA size fractions.

3.2. Penetration of water under pressure

Three 150 mm cubes for each prepared mix were exposed to water under the pressure of 5 bars for 72 h. When a leakage of water was observed during the test from the side wall of the cube (see an example in Fig. 4), the test on that cube was terminated. This was the case for all the SCLC1 and SCLC2 cubes during the first hours of testing, and therefore these mortars can be classified as highly permeable. Significantly different results were obtained on VCLC cubes, for which only very shallow water penetration fronts were observed, with an average penetration depth of 6.4 mm after 72 h test. This shallow penetration depth reflects a very low permeability of VCLC. Fig. 5 shows examples of the water penetration fronts measured on split cubes after performing the water pressure penetration test. These results suggest that, despite the fact that the measured water-permeable porosities were comparable for all the prepared mortars (30% for VCLC and about 35% for SCLC1 and SCLC2), mixture VCLC is significantly less permeable compared to the very permeable mixtures SCLC1 and SCLC2. For the VCLC, the water under pressure applied during the test could not permeate the mortar as efficiently as during the vacuum-saturation technique (applied under pressure of 40 mbar) used for the measurement of the water-permeable porosity. Because there were only coarse LWA particles in VCLC embedded in a dense cement paste with impermeable fillers (normal density sand and microsand), their internal pores were not permeable to water under the pressure of 5 bar. Apparently, water at this pressure could not be pushed sufficiently hard inside to overcome the resistance of the fine pore structure. Therefore, a large fraction of the LWA-pores in the VCLC mix which were permeable to water under vacuum-conditions, were impermeable to water under the pressure of 5 bar. A different conclusion can be drawn analyzing the results obtained on mortars SCLC1 and SCLC2, where the pores of the hardened paste and the internal pores in LWA were well interconnected and therefore, the overall water permeability of these composites was very high.

3.3. Capillary water absorption

The 28 days capillary absorption was calculated as follows:

$$C_A = \frac{m_{28} - m_0}{a^2} \quad (1)$$

where C_A – capillary absorption index, m_{28} – mass of sample after 28 days of exposure to water, m_0 – initial mass of the sample after 28 days of curing and a^2 – cross-section area of the sample.

Table 2
Computed porosities of the hardened cement paste ($\varphi_{v,paste}$), LWA ($\varphi_{v,LWA}$), mortar (φ_v) and the measured water-permeable porosities ($\varphi_{v,p}$).

Mixture	$\varphi_{v,paste}$ (%)	φ_{paste} (dm^3/m^3)	$\varphi_{v,LWA}$ (%)	φ_{LWA} (dm^3/m^3)	φ_v (%)	$\varphi_{v,p}$ (%)
SCLC1	39.71	384.6	79.73	404.2	47.50	34.31
SCLC2	36.18	363.5	79.25	318.7	38.40	34.97
VCLC	21.47	291.4	86.67	412.6	42.01	30.65

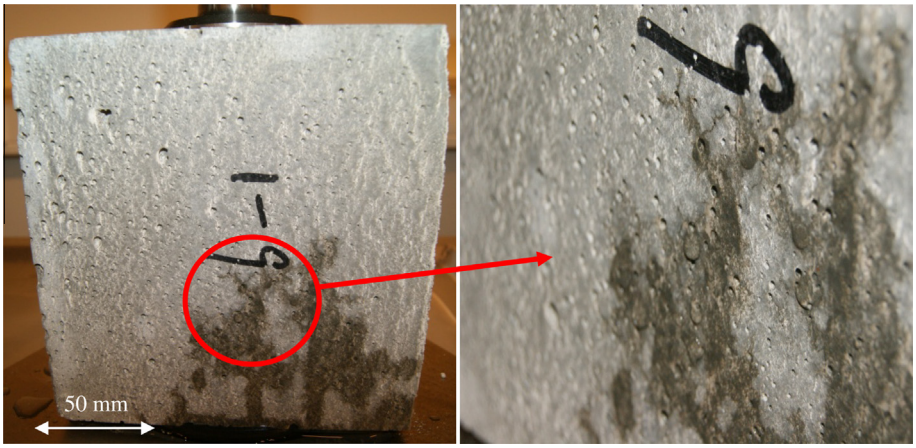

Fig. 4. Penetration of water observed during the water pressure permeability test.

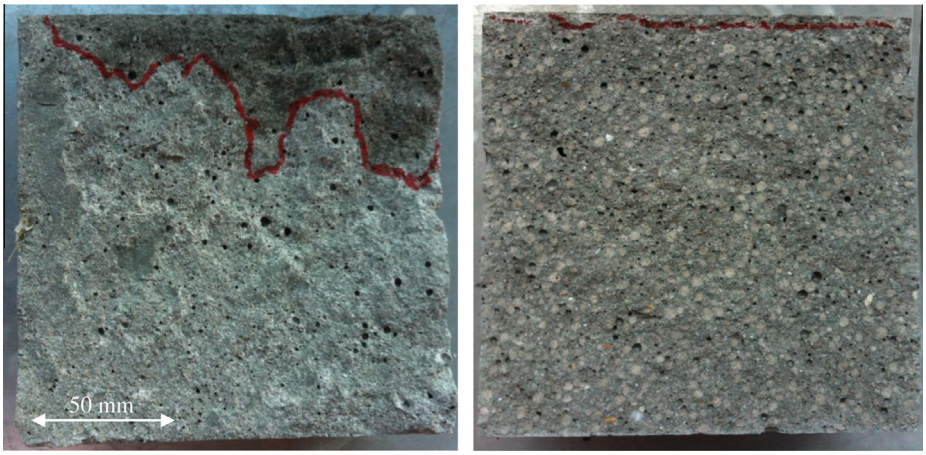

Fig. 5. Split surfaces of cubes after the water pressure permeability test; water ingress from the side of the top surface. (a) SCLC2 and (b) VCLC.

The obtained values of C_A are shown in Table 3. The evolution of the mass of the samples due to the water absorption is shown in Fig. 6. As can be seen, the mass increase was larger for the SCLC1 and SCLC2 samples, which confirms the previously discussed findings that in these composites the water-permeable porosity and the connectivity of the pores were larger compared to the VCLC mix. From these results it becomes also clear that the connectivity of the internal LWA pores within the mortar SCLC2 is larger than in SCLC1, as it could absorb more water. This is in line with the findings presented in Section 3.1, showing that a larger fraction of the internal LWA pores remains closed in SCLC1 than in SCLC2.

3.4. Freeze–thaw test

The freeze-thaw test was performed in 56 cycles, during which the surface scaling was measured after 14, 28 and 56 cycles respectively. Fig. 7 shows a picture of the exposed surfaces of the test samples after 56 freeze–thaw cycles.

A visual comparison of the surfaces of the mortars exposed to 56 freeze–thaw cycles reflects their excellent freeze–thaw resistance. This resistance is much better for the developed LWA mortars (a–c in Fig. 7) than for a high performance, normal density SCC sample (d in Fig. 7), shown as a reference. In Table 4 an average integral surface scaling (S_n) after 56 cycles is given. The increased porosity of the mortars helps to avoid the micro-damage caused by the crystallization of ice. Following the classification of resistance of concrete against the freeze–thaw damage given in [24], all the developed composites can be classified as having a very good freeze–thaw resistance, as the total amount of the surface-scaled material after 56 cycles is lower than 100 g/m^2. Furthermore, the obtained values are by far lower than given for this most strict classification. Additionally, comparing the S_n of each prepared composite, it can be seen that the samples with larger porosity and connectivity of the pores (SCLC1 and SCLC2) show better scaling resistance compared to the samples with a lower porosity and connectivity (VCLC).

3.5. Alkali-silica reaction and SEM analyses of the microstructure

Application of glass in cementitious systems brings up a possibility of the alkali-silica reaction (ASR), which in time may lead to the deterioration of concrete. The lightweight aggregates used in this study were produced from recycled glass, and therefore can react with the alkalis originating from the cement. The ASR in glass-LWA concrete was extensively investigated in literature, but the outcome of these research is contradictory, stating that the ASR does not appear [25], appears without causing any damage as

Table 3
Capillary absorption index (C_A) of tested samples.

Mixture	C_A (g/mm^2)							Standard
	1	2	3	4	5	6	Average	deviation
SCLC1	0.0075	0.0084	0.0079	0.0073	0.0070	0.0068	0.0075	0.0005
SCLC2	0.0126	0.0129	0.0140	0.0161	0.0145	0.0138	0.0140	0.0011
VCLC	0.0050	0.0050	0.0049	0.0044	0.0043	0.0053	0.0048	0.0004

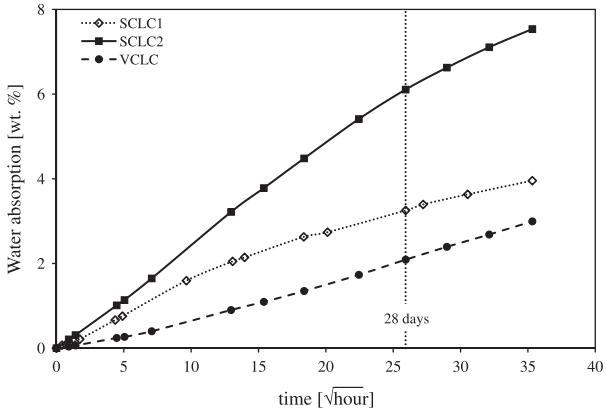

Fig. 6. Water absorption of mortar prisms in time.

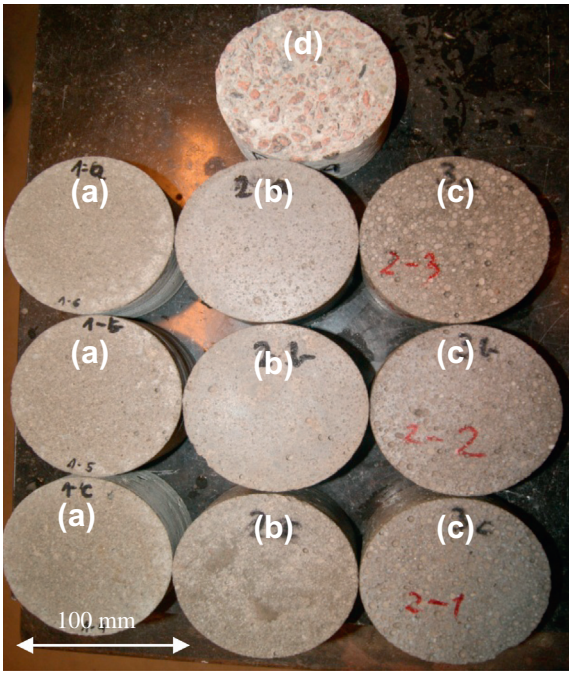

Fig. 7. Surface of lightweight mortar samples after 56 freeze–thaw cycles. (a) SCLC1, (b) SCLC2, (c) VCLC and (d) high performance self-compacting concrete as a reference.

the ASR products are formed in the pores [26,27] or appears and causes structural damage [28].

The presence of the ASR reaction was explored in the present study by analyzing the interface zone between the LWA and hardened cement paste. In the case of the ASR in LWA concrete, characteristic rings (reaction products) would be visible around the LWA. As can be seen in Fig. 8, obtained using a SEM microscope in backscattered electron mode, there are no reaction products at the interface. Therefore, it can be concluded that, until the time when the samples were inspected (up to 20 months after casting), there were no ASR products. Additionally, as can be seen in Fig. 8, the interface zone between the LWA and the cement paste is dense and homogenous (no air bubbles or other inclusions are present).

3.6. Electrical resistivity

A higher resistivity of concrete/mortar reflects on a lower porosity and connectivity of the pores. Similarly to the penetration of water under pressure and to the capillary water absorption tests, the resistivity of liquid-saturated mortars reflects their porosity and connectivity of the pores. The measured resistivity (R) of the samples is shown in Table 4, where the average values obtained on three samples for each type of mortar are presented. These results are in line with the findings from the previously discussed experiments, showing that the self-compacting composites SCLC1 and SCLC2 have larger porosity and connectivity of pores compared to VCLC. Following the recommendations given in [29] for the assessment of the risk of corrosion of steel-reinforced Ordinary Portland Cement (OPC) concrete, for the resistivity <100 Ωm the risk of chloride-induced corrosion of the reinforcing steel is high (this is the case for mixes SCLC1 and SCLC2), while for the mix VCLC it is moderate, in the range of 100–500 Ωm.

3.7. RCM and chloride diffusion tests

A detailed RCM test procedure as well as the calculation method for the chloride migration coefficient D_{RCM} is presented in [9,17,30]. The results (average of three measurements) of the RCM test performed at the ages of 28 and 91 days are shown in Table 4. The obtained chloride migration coefficients follow the same trend as the one observed in the other experiments: larger values of the migration coefficients, reflecting larger porosity and connectivity of pores, were obtained on the SCLC1 and SCLC2 samples while the lowest were obtained for VCLC, regardless of the age of the samples at the testing time.

A quantification of the resistance of concrete against the ingress of chlorides based on the 28 days D_{RCM} is given in [31], which is based on the DuraCrete model for service life of concrete [32]. In Table 5 the maximum values of the D_{RCM} are shown for 100 years of service-life design, considering the exposure class (XS – exposure to chloride originating from seawater and XD – exposure to chlorides originating from sources other than seawater) [33], type of used cement, type of the reinforcing steel and depth of the concrete cover.

Comparing the obtained 28 days D_{RCM} given in Table 4 to the recommendations given in Table 5, it can be seen that the mixture SCLC1 can provide 100 years of service life of concrete/mortar elements in the exposure classes XD1, XD2, XD3 and XS1 with a cover depth of at least 60 mm (70 mm in the case of pre-stressed reinforcing steel). For the other exposure classes, the permeability of this mortar is too large for the considered cover depths. A significant improvement of the D_{RCM} is observed in the case of mix VCLC.

Table 4
Results of measurements of resistivity (R), chloride migration (D_{RCM}) and diffusion coefficients (D_{app}) and freeze–thaw surface scaling (S_n) for the developed lightweight composites; standard deviations in brackets.

Mixture	R (Ωm)	D_{RCM} 28 days ($\cdot 10^{12}$ m^2/s)	D_{RCM} 91 days ($\cdot 10^{12}$ m^2/s)	D_{app} ($\cdot 10^{12}$ m^2/s)	S_n 56 cycles (g/m^2)
SCLC1	34.1 (2.9)	20.63 (1.52)	9.08 (0.85)	12.30	21.4 (5.1)
SCLC2	32.2 (3.6)	>29[a]	15.38 (1.31)	18.00	23.9 (2.9)
VCLC	140.2 (5.4)	4.04 (0.21)	3.48 (0.35)	3.76	28.3 (4.8)

[a] Samples failed in the test (chloride breakthrough observed).

This mix can be used with a cover layer of 40 mm for the exposure classes XD1, XD2, XD3 and XS1 and 50 mm of cover for the exposure classes XS2 and XS3. In the case of composite SCLC2, the 28 days D_{RCM} could not been determined accurately, because during the RCM test the chlorides penetrated the entire volumes of the samples. Therefore for the computation of the D_{RCM} of SCLC2 the chloride penetration depth equal to the thickness of the sample (0.05 m) was used. The obtained values confirm again that this mixture has the largest permeability among all the mixtures developed in this study. The 91 days D_{RCM}, shown in Table 4, are smaller than the 28 days values, which can be attributed to a densification of the matrix due to the progressing hydration of cement. Nevertheless, the same trend between the values can be observed: the 91 days D_{RCM} for VCLC is much smaller compared to the ones for SCLC1 and SCLC2.

As explained earlier in this study, the permeability of the composite can be considered as a function of the applied liquid intrusion technique. The RCM test is always performed on samples vacuum-saturated with limewater and therefore the accessible pores are liquid-saturated. On the other hand, in the case of a real exposure to external chlorides (seawater or de-icing salts), the material is never vacuum-saturated but only 'naturally' exposed to a chloride solution. Additionally, the chlorides do not penetrate the material by means of the electro-migration but only by the diffusion and/or capillary suction. This case is represented in the chloride diffusion tests such as the NT Build 443 [18]. Therefore, the chloride diffusion test was performed in this study as a reference to the accelerated RCM test.

The results of the diffusion test are shown in Table 4 and in Fig. 9. The obtained values of the chloride diffusion coefficients D_{app} correspond well with the chloride migration coefficients obtained from the RCM test, classifying again the permeability of the developed composites in the descending order: SCLC2, SCLC1 and VCLC, respectively.

3.8. Discussion

The water-permeable porosity of the developed lightweight mortars was measured and compared to the estimated total porosity, showing that a certain fraction of internal LWA pores remains closed. These pores contribute to the total porosity of the composite but do not facilitate the transport process of water or aggressive

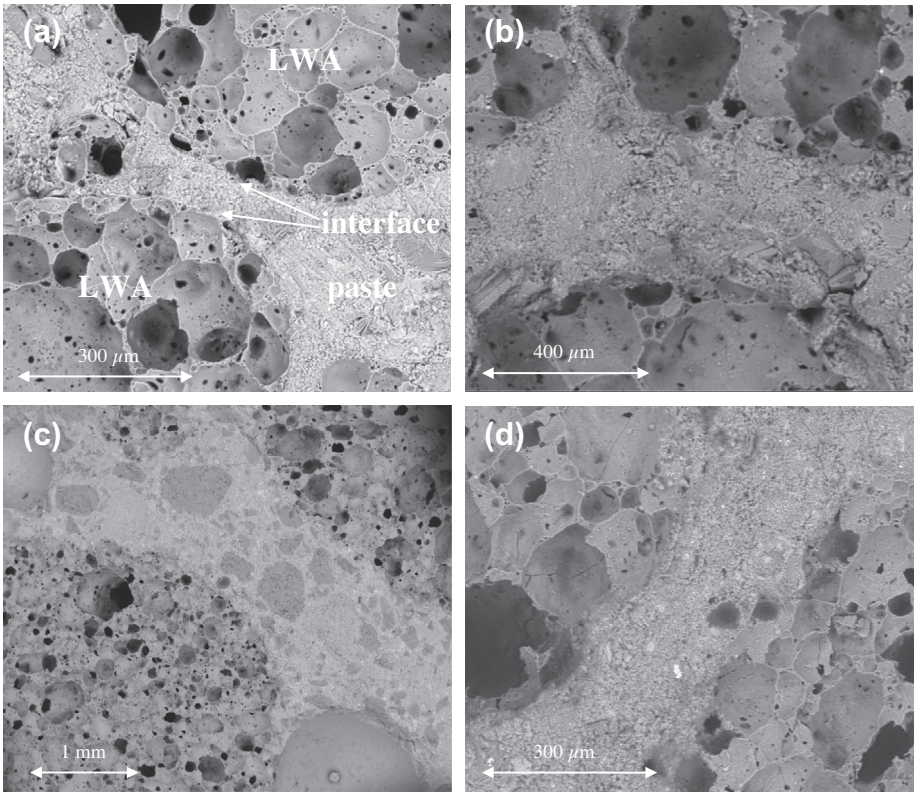

Fig. 8. SEM pictures of the LWA/cement paste interface; (a) SCLC1 after 2 months of curing, (b) SCLC1 after 20 months of curing, (c) VCLC after 2 months of curing and (d) VCLC after 20 months of curing.

Table 5
Maximum values of 28 days D_{RCM} for 100 years of service-life design of concrete [31].

Minimum concrete cover depth (mm)		Maximum value of D_{RCM} ($\cdot 10^{12}$ m^2/s)							
Steel	Pre-stressed steel	CEM I		CEM III, CEM I + 25–50% GGBS		CEM III 50–80% GGBS		CEM II B/V, CEM I + 20–30% fly ash	
		XD1, XD2, XD3, XS1	XS2, XS3	XD1, XD2, XD3, XS1	XS2, XS3	XD1, XD2, XD3, XS1	XS2, XS3	XD1, XD2, XD3, XS1	XS2, XS3
35	45	3.0	1.5	2.0	1.0	2.0	1.0	6.5	5.5
40	50	5.5	2.0	4.0	1.5	4.0	1.5	12	10
45	55	8.5	3.5	6.0	2.5	6.0	2.5	18	15
50	60	12	5.0	9.0	3.5	8.5	3.6	26	22
55	65	17	7.0	12	5.0	12	5.0	36	30
60	70	22	9.0	16	6.5	15	6.5	47	39

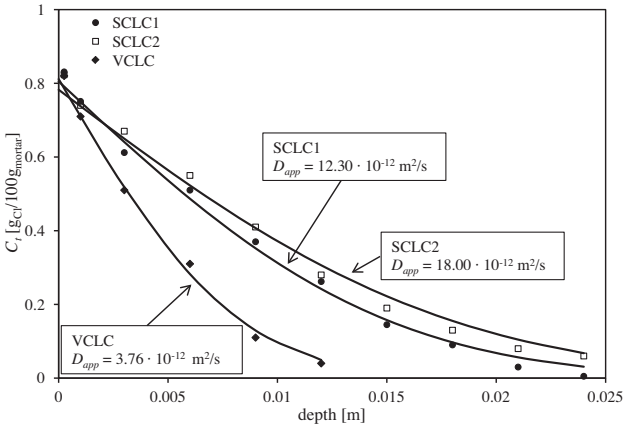

Fig. 9. Chloride diffusion profiles and obtained chloride diffusion coefficients (D_{app}).

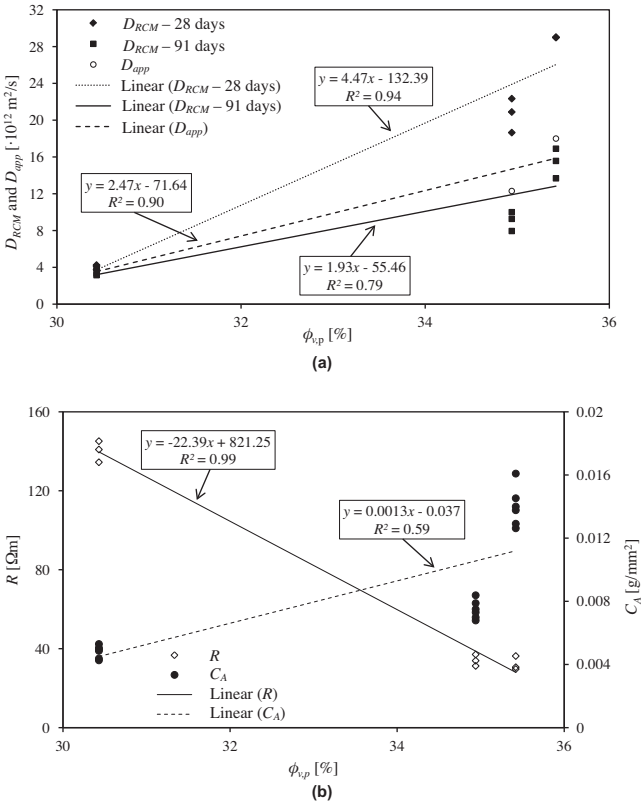

Fig. 10. Relationship between the water-permeable porosity and (a) chloride diffusion and migration coefficients and (b) resistivity and capillary water absorption index.

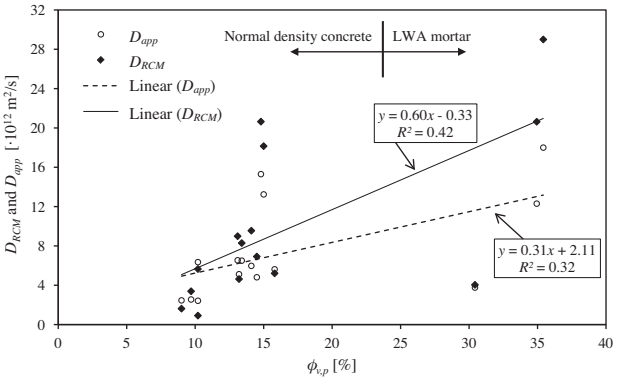

Fig. 11. Relationship between the chloride transport properties (D_{app} and D_{RCM}) of the LWA mortars and normal density concretes vs. their water-permeable porosities ($\varphi_{v,p}$). The data for the normal density concrete retrieved from [19].

substances. Comparing the three developed mixtures, the most successful (the least permeable) material was composed of a good quality cement paste (low *w/c* ratio and therefore a reduced paste porosity) together with normal density sand and only coarse fractions of LWA (1–4 mm). This is in line with [4,5], where it was shown that the quality of the hardened cement paste plays the most crucial role in the permeability of LWA concrete. The two self-compacting LWA composites developed here were found to be very permeable and this can be explained by the combination of a permeable cement paste in these mixes (high *w/c* ratios) and by the application of large volumes of fine LWA. Apparently, it is much easier for the permeating liquid to find a path through the fine LWA particles than through larger aggregates. Such a conclusion is in agreement with [5,6], where the LWA sand was identified to significantly increase the permeability of LWA concrete.

Various permeability tests performed in this study showed exactly the same trend: the permeability of both developed self-compacting LWA mortars was much larger compared to the vibrated mortar. Additionally, because the amount of the finest LWA size fraction (0.1–0.3 mm) was larger in SCLC2, the permeability of this composite was higher compared to that of SCLC1.

In Fig. 10a the obtained chloride diffusion (D_{app}) and migration (D_{RCM}) coefficients are plotted against the measured water-permeable porosities ($\varphi_{v,p}$) of the developed LWA mortars, showing fairly linear trends. This indicates that the water-permeable porosity plays an important role in the chlorides ingress speed into cement-based lightweight composites. The capillary water absorption index (C_A) can also be related to the water-permeable porosity, but as Fig. 10b shows, this relation is not straightforward. It can be explained by the fact that the capillary water absorption is not only a function of the volume of the accessible pores, but also of the pore structure (i.e. diameter of pores, tortuosity and constrictivity) and their connectivity.

As can be seen in Fig. 10b, the resistivity of saturated mortars (R) can be linearly correlated with the water-permeable porosity. This linear relationship means that, when the chemical composition of the pore solution is the same (this can be assumed as all

Table 6
Mixture proportions and properties of normal density OPC concretes retrieved from [19].

Material	M1 (kg/m^3)	M2 (kg/m^3)	M3 (kg/m^3)
CEM I 52.5 N	363	380	400
Gravel	1162	1217	1281
Sand	599	627	660
Water	218	182	140
Superplasticizer (wt.% of cement)	–	–	1
Water/cement ratio	0.60	0.48	0.35
Dry density (kg/m^3)	2247	2286	2393
56 days compressive strength (N/mm^2)	37.9	46.7	81.7
$\varphi_{v,p}$ (%)	15.0	14.1	10.2

Table 7
Porosities and chloride transport properties of lightweight mortars and normal density concretes.

Mixture	$\varphi_{v,paste}$ (%)	φ_{paste} (dm^3/m^3)	$\varphi_{v,paste'}$ (%)	$\varphi_{v,p}$ (%)	D_{RCM} ($\cdot 10^{12}$ m^2/s)	D_{app} ($\cdot 10^{12}$ m^2/s)
M1	40.37	333.2	13.41	15.0	18.15	13.24
M2	31.36	302.6	11.40	14.1	9.55	5.97
M3	17.92	267.0	5.22	10.2	5.65	6.35
SCLC1	39.71	384.6	19.90	34.31	20.63	12.3
SCLC2	36.18	363.5	18.81	34.97	>29	18
VCLC	21.47	291.4	6.26	30.65	4.04	3.76

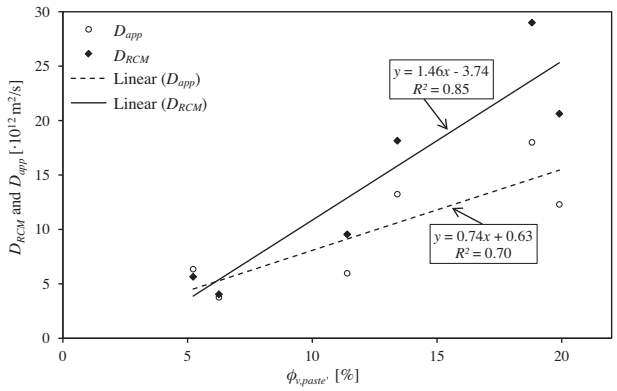

Fig. 12. Relationship between the chloride transport properties (D_{app} and D_{RCM}) of lightweight mortars and normal density concretes vs. their paste porosities including the porosity of the 0.1–0.3 mm fraction of LWA ($\varphi_{v,paste'}$).

the samples were tested at the same age and the same type of cement was used), the resistivity of the composite is controlled by its permeable porosity.

As shown in Fig. 10a, the chloride diffusion and migration coefficients for the developed lightweight composites are proportional to the water-permeable porosity ($\varphi_{v,p}$). However, when extending the water-permeable porosity spectrum to normal density concretes, this relationship is not obeyed anymore as Fig. 11 shows, in which data retrieved from [19] is incorporated. This data includes the values obtained on normal density concretes prepared with CEM I 52.5N and silica fume, fly ash or granulated blast furnace slag (GGBS), in the permeable porosity range of 8–16%. As can be seen in Fig. 11, for both D_{app} and D_{RCM} in the permeable porosity range of 8–36%, the linear fit is obeyed rather poorly (R^2 of 0.32 and 0.42 respectively). This gives evidence that the water-permeable porosity is not the main factor determining the chloride transport properties in the case of a broad spectrum of concrete/mortar porosities.

Table 6 shows the mixture composition and some other properties of three normal density OPC concretes (M1, M2 and M3) retrieved from [19]. The type of cement and the technique for determining the water-permeable porosity were the same as used in the present study. Table 7 presents the porosities of the cement paste ($\varphi_{v,paste}$) of mixes M1, M2 and M3, calculated from the modified Powers and Brownyard model (see Part 1 [1]), volume fractions of the cement paste in concrete (φ_{paste}) and water-permeable porosities ($\varphi_{v,p}$). The porosities of concretes (M1, M2 and M3), and lightweight mortars (SCLC1, SCLC2 and VCLC) contributed by their paste fractions to the total porosity are also given in Table 7 as $\varphi_{v,paste'}$. This porosity consists of the capillary pores present in the hardened cement paste and the pores originating from the finest size fraction of the LWA (i.e. LWA 0.1–0.3 mm used in SCLC1 and SCLC2), as it has been shown that this fraction could also be permeable. When plotting the D_{app} and D_{RCM} of the LWA mortars and normal density concretes against the porosities contributed by their pastes, a fairly linear trend can be observed, as shown in Fig. 12. This trend is clearer than the trend between the chloride diffusion/migration coefficient and the water-permeable porosities, given in Fig. 11. Such a clear relationship confirms that the transport of liquids in the investigated materials is governed by the porosity of the paste (capillary porosity in the case of normal density concrete and capillary porosity plus the porosity of the 0.1–0.3 mm LWA in the case of the LWA mortars) rather than the total water-permeable porosity. This also means that in the case of the analyzed LWA composites, the coarser lightweight aggregates do not participate in the transport process of liquids. Therefore, the absence of the smallest size LWA fraction combined with a low porosity of the hardened cement paste explains the excellent permeability test results obtained for the developed vibrated lightweight composite (VCLC).

4. Conclusions

This article presents an investigation on the durability-related properties of the lightweight composites. Expanded glass lightweight aggregates (LWAs) were applied in the lightweight composites. The following conclusions can be drawn:

- The design approach followed in this study for the LWA composites allows for the design targeted on the strength, density, thermal conductivity and permeability, or their combination.
- The difference between the total porosity and the measured water-permeable porosity indicates that the used LWA have a certain amount of closed internal pores, which will contribute to a lower density and better thermal insulation of the composite, but will not facilitate the transport of liquids.
- Application of fine size fractions of LWA (especially the 0.1–0.3 mm fraction) in a combination with high *w/c* ratios significantly increases the overall permeability of the composites.
- Cement paste with a low capillary porosity significantly reduces the permeability of the LWA composites as the number of the interconnections between the LWA particles is limited. The porosity of the hardened paste (hydrated cement and, if present, LWA size fraction <0.3 mm) governs the chloride transport properties of the designed LWA composites as well as normal density concretes.

- All the developed mortars have excellent resistance to the freeze–thaw induced damage.
- No traces of alkali-silica reactions were found at the interface of the expanded glass LWA/cement paste. Good adhesion of the paste to the LWA was observed. In the case of LWA particles, this can reduce their permeability.

Acknowledgements

The authors wish to express their gratitude to Dipl. Eng. M.V.A. Florea for her help and to the following sponsors of the Building Materials research group at TU Eindhoven: Rijkswaterstaat Centre for Infrastructure, Graniet-Import Benelux, Kijlstra Betonmortel, Struyk Verwo, Attero, Enci, Provincie Overijssel, Rijkswaterstaat Directie Zeeland, A&G Maasvlakte, BTE, Alvon Bouwsystemen, V.d. Bosch Beton, Selor, Twee "R" Recycling, GMB, Schenk Concrete Consultancy, Geochem Research, Icopal, BN International, APP All Remove, Consensor, Eltomation, Knauf Gips, Hess AAC Systems, Kronos and Joma International (in chronological order of joining).

References

[1] Yu QL, Spiesz P, Brouwers HJH. Development of cement-based lightweight composites – Part 1: Mix design, strength and thermal properties. Cem Concr Compos 2013;44:17–29.
[2] Neville AM. Properties of concrete. 4th ed. Essex, England: Pearson Educational Limited; 2002. [ISBN: 978-0-582-23070-5].
[3] EuroLightCon. LWAC material properties state-of-the-art. In: Economic design and construction with light weight aggregate concrete. Brite-EuRam III; 1998.
[4] Liu X, Chia KS, Zhang M-H. Development of lightweight concrete with high resistance to water and chloride-ion penetration. Cem Concr Compos 2010;32:757–66.
[5] Chia KS, Zhang M-H. Water permeability and chloride penetrability of high-strength lightweight aggregate concrete. Cem Concr Res 2002;32:639–45.
[6] Nyame BK. Permeability of normal and lightweight mortars. Mag Concr Res 1985;37(130):44–8.
[7] Bentz DP. Influence of internal curing using lightweight aggregates on interfacial transition zone percolation and chloride ingress in mortars. Cem Concr Compos 2009;31:285–9.
[8] Liu X, Chia KS, Zhang M-H. Water absorption, permeability, and resistance to chloride-ion penetration of lightweight aggregate concrete. Constr Build Mater 2011;25:335–43.
[9] NT Build 492. Concrete, mortar and cement-based repair materials: chloride migration coefficient from non-steady-state migration experiments. Nordtest method, Finland; 1999.
[10] ASTM C1202. Standard Test Method for Electrical Indication of Concrete's Ability to Resist Chloride Ion Penetration. In: Annual Book of ASTM Standards, vol. 04.02. Philadelphia: American Society for Testing and Materials; July 2005.
[11] Safiuddin M, Hearn N. Comparison of ASTM saturation techniques for measuring the permeable porosity of concrete. Cem Concr Res 2005;35:1008–13.
[12] ASTM C 642-97. Standard Test Method for Density, Absorption, and Voids in Hardened Concrete.
[13] BS-EN 12390-8. Testing hardened concrete – depth of penetration of water under pressure. British Standards Institution-BSI and CEN European Committee for Standardization; 2009.
[14] DIN-EN 480-5. Admixtures for concrete mortar and grout – test methods – Part 5: Determination of capillary absorption; 2005 [in German].
[15] NEN-EN 12390-9. Testing hardened concrete – Freeze–thaw resistance – Scaling. CEN European Committee for Standardization and Dutch Normalization-Institute, Delft, the Netherlands; 2006 [in English].
[16] Polder RB. Test methods for on site measurement of resistivity of concrete – a RILEM TC-154 technical recommendation. Constr Build Mater 2001;15:125–31.
[17] Spiesz P, Brouwers HJH. Influence of the applied voltage on the Rapid Chloride Migration (RCM) test. Cem Concr Res 2012;42:1072–82.
[18] NT Build 443. Concrete, hardened: accelerated chloride penetration. Nordtest method. Finland; 1995.
[19] Yuan Q. Fundamental studies on test methods for transport of chloride ions in cementitious materials. PhD thesis, University of Gent, Belgium; 2009.
[20] Elsharief A, Cohen MD, Olek J. Influence of lightweight aggregate on microstructure and durability of mortar. Cem Concr Res 2005;35:1368–76.
[21] Brouwers HJH. The work of Powers and Brownyard revisited: Part 1. Cem Concr Res 2004;34:1697–716.
[22] Brouwers HJH. The work of Powers and Brownyard revisited: Part 2. Cem Concr Res 2005;35:1922–36.
[23] Powers TC, Brownyard TL. Studies of the physical properties of hardened Portland cement paste, Bull 22, Res Lab of Portland Cement Association, Skokie, IL, USA, reprinted from J Am Concr Inst (Proc), 1947:43.
[24] SS 437244. Concrete testing – hardened concrete – frost resistance. Borås method, Stanardieringskommissionen i Sverige; 1992 [in Swedish].
[25] Lindgård J, Andiç-Çakır Ö, Fernandes I, Rønning TF, Thomas MDA. Alkali-Silica Reactions (ASRs): literature review on parameters influencing laboratory performance testing. Cem Concr Res 2012;42:223–43.
[26] Ducman V, Mladenovič A, Šuput JS. Lightweight aggregate based on waste glass and its alkali-silica reactivity. Cem Concr Res 2002;32:223–6.
[27] Mladenovič A, Šuput JS, Ducman V, Škapin AS. Alkali-silica reactivity of some frequently used lightweight aggregates. Cem Concr Res 2004;34:1809–16.
[28] Matsuda Y, Tsuyoshi T, Ishibashi T. Investigation of Real Structures using lightweight concrete. In: Upgrade symposium on concrete repair and reinforcement, Kyoto, Japan; 2004. p. 183–8.
[29] COST 509. Corrosion and protection of metals in contact with concrete. Final report. In: Cox R, Cigna R, Vannesland O, Valente T, editors. European commission, directorate general science, research and development, Brussels, EUR 17608 EN; 1997. [ISBN 92-828-0252-3].
[30] Spiesz P, Ballari MM, Brouwers HJH. RCM: a new model accounting for the non-linear chloride binding isotherm and the non-equilibrium conditions between the free- and bound-chloride concentrations. Constr Build Mater 2012;27:293–304.
[31] CUR Durability Guideline. Duurzaamheid van constructief beton met betrekking tot chloride-geïnitieerde wapeningscorrosie. CUR Bouw en Infra, Gouda, the Netherlands; 2009 [in Dutch].
[32] DuraCrete. Probabilistic Performance based Durability Design of Concrete Structures. DuraCrete Final Technical Report. Document BE95-1347/R17; 2000.
[33] NEN-EN 206-1. Concrete – Part 1: Specification, performance, production and conformity. CEN European Committee for Standardization and Dutch Normalization-Institute, Delft, the Netherlands; 2000 [in English].